ChemComm

REVIEW ARTICLE

View Article Online
View Journal

Cite this: DOI: 10.1039/d6cc01709f

Computational modeling of electrocatalyst reconstruction

Ziyan Liu and Xiao-Yan Li *

Electrocatalyst reconstruction under operating conditions is now widely recognized as a key factor governing catalytic activity, selectivity, and stability. Substantial progress has been made in developing computational methods to describe this structurally dynamic behavior, ranging from density functional theory-based phase diagram analysis to global structure search, *ab initio* molecular dynamics, kinetic Monte Carlo, and machine learning-accelerated simulations. In this Review, we provide a concise overview of how these approaches have advanced the mechanistic understanding of electrocatalyst reconstruction across multiple time and length scales. We highlight how different computational strategies offer complementary insights into thermodynamically accessible states, atomic-scale restructuring pathways, and kinetically relevant structural evolution under reaction conditions. We emphasize the recent progress in machine learning potentials and multiscale modeling frameworks, which are extending simulations towards increasingly realistic chemical complexity. We also discuss the key challenges that remain, especially the need for open-system models that explicitly account for interfacial exchange, dissolution–redeposition processes, and the coupling between the local chemical environment and structural dynamics. This Review aims to provide a practical guide to the current computational toolbox and to outline directions for the next generation of predictive modeling for electrocatalyst reconstruction.

Received 21st March 2026,
Accepted 14th May 2026

DOI: 10.1039/d6cc01709f

rsc.li/chemcomm

1 Introduction

Electrocatalysis plays a central role in sustainable chemical transformation, including water splitting,[1,2] carbon dioxide reduction,[3,4] nitrogen conversion,[5,6] and electro-organic synthesis.[7,8] In these systems, catalyst performance is traditionally interpreted in terms of static structure–activity relationships, where a well-defined surface or active site is assumed to govern the reaction. Over the past decade, however, it has become increasingly clear that many electrocatalysts do not remain structurally unchanged under operating conditions. Instead, they undergo continuous or potential-dependent

Department of Chemistry, National University of Singapore, 3 Science Drive 3, 117543, Singapore. E-mail: xiaoyanli@nus.edu.sg

Ziyan Liu

Ziyan Liu is a PhD student in the Department of Chemistry at the National University of Singapore under the supervision of Prof. Xiaoyan Li. He received his BS degree at Dalian University of Technology in 2022 and MS degree in Chemical Engineering at Tianjin University in 2025. His research mainly focuses on AI/ML-assisted computational simulation for catalyst reconstruction in reactions.

Xiao-Yan Li

Xiaoyan Li is an assistant professor in the Department of Chemistry at the National University of Singapore, starting from August 2025. Dr Li received her PhD degree in June 2021 from the Shanghai Institute of Applied Physics, University of Chinese Academy of Sciences. From 2021–2025, she conducted postdoctoral research under the supervision of Prof. Edward H. Sargent at the University of Toronto in Canada and at Northwestern University in the United States of America.

reconstruction, driven by the coupled effects of electrode potential,[9] adsorbates,[10] electrolyte composition,[11] local pH,[12] dissolution-redeposition processes,[13] and interfacial mass transport.[14] As a result, the catalytically relevant state is often not the as-synthesized material, but a dynamic ensemble of metastable structures that evolves during operation.[15,16]

In CO_2 electro-reduction, for example, the Cu-based catalyst surface can reconstruct into dynamic motifs with distinct product selectivity.[17–19] Similar behavior is also observed in other alloy catalysts, where adsorbate coverage affected by the electrochemical bias can induce component segregation and reconfigure active ensembles, thereby altering catalytic pathways.[20] In metal oxides, hydroxylation[21] and lattice distortion[22] under reaction conditions can likewise generate interfacial motifs that differ from the bulk termination and reshape the catalytic landscape. Accurately recognizing and controlling reconstruction is therefore essential for establishing predictive structure–activity-stability relationships in electrocatalysis. Despite significant advances in *operando* and *in situ* techniques, capturing reconstruction pathways in real time with atomic-level specificity remains highly challenging. Transient states are short-lived, competing pathways can be closely balanced, and the relevant observables often couple structure, composition, and local environment.[23,24]

These practical challenges make computational modeling approaches uniquely valuable, not only as a complement to experiments, but also as a route toward mechanistic interpretation and predictive modeling. Density functional theory (DFT)-based electrochemical phase diagrams, for example, provide potential-pH-dependent stability maps that rationalize which bulk and surface states are thermodynamically preferred.[25–27] More recently, machine learning potentials (MLPs) and data-driven sampling strategies have started to extend atomistic simulations towards larger configurational spaces, longer time scales, and more chemically complex environments.[28–32] Together, these developments are making it increasingly possible to explore not only what reconstructed states are stable, but also how they form, evolve, and interconvert under realistic operating conditions.

In this Review, we provide a concise summary of computational approaches for studying electrocatalyst reconstruction across scales (Fig. 1). We first summarize the thermodynamic frameworks used to map reconstructed states under electrochemical conditions, including phase-diagram-based analyses and related formalisms. We then discuss atomistic and dynamic approaches, such as global structure search, AIMD, and kMC, for uncovering reconstruction pathways and kinetic evolution. Next, we highlight recent progress in MLP-enabled and multiscale frameworks that bridge configurational complexity, kinetics, and realistic chemical environments. Finally, we outline key challenges and opportunities for the next generation of predictive modeling, particularly the need for open-system approaches that explicitly couple structural dynamics with electrochemical operating conditions.

2 Methodological framework for reconstruction studies

2.1 Thermodynamic mapping and configurational exploration of reconstruction

Electrocatalyst reconstruction typically involves intricate transitions between various structural states under reaction conditions, such as applied potential, pH, and adsorbate coverage. Therefore, it is necessary to identify which structural phases in the bulk or on the surface exist under a given electrochemical environment.[33–37] From a thermodynamic perspective, phase diagrams provide an effective way to condense this complexity involving structure and conditions into an interpretable map of thermodynamic stability, revealing which structural motif prevails under the corresponding conditions.[38,39]

Representative bulk phase map studies by Sun *et al.* have illustrated the thermodynamic role of this approach in nanomaterial reconstruction analysis. As shown in Fig. 2a,[33] the Pourbaix diagram of Mn oxides derived from DFT calculations exhibits that even within the same stability region, subtle variations in pH and redox potential can redirect a non-equilibrium crystallization pathway through different metastable intermediates.

At the interface, surface state maps more directly describe the interfacial states where electrocatalytic reactions occur.

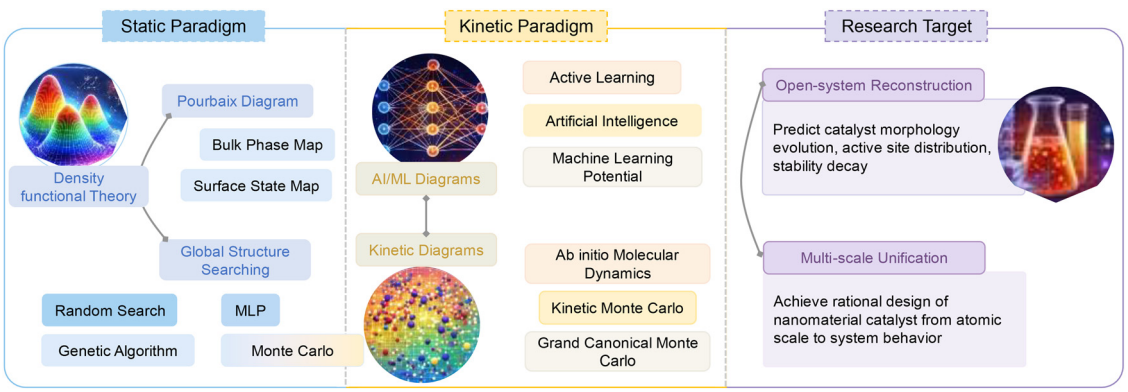

Fig. 1 Schematic workflow of computational toolkits for electrocatalyst reconstruction, linking potential/pH-dependent thermodynamic maps and global structure search to kinetic simulations (AIMD, GCMC, kMC) and ML-accelerated exploration, toward active state identification and activity–stability predictions under operating conditions.

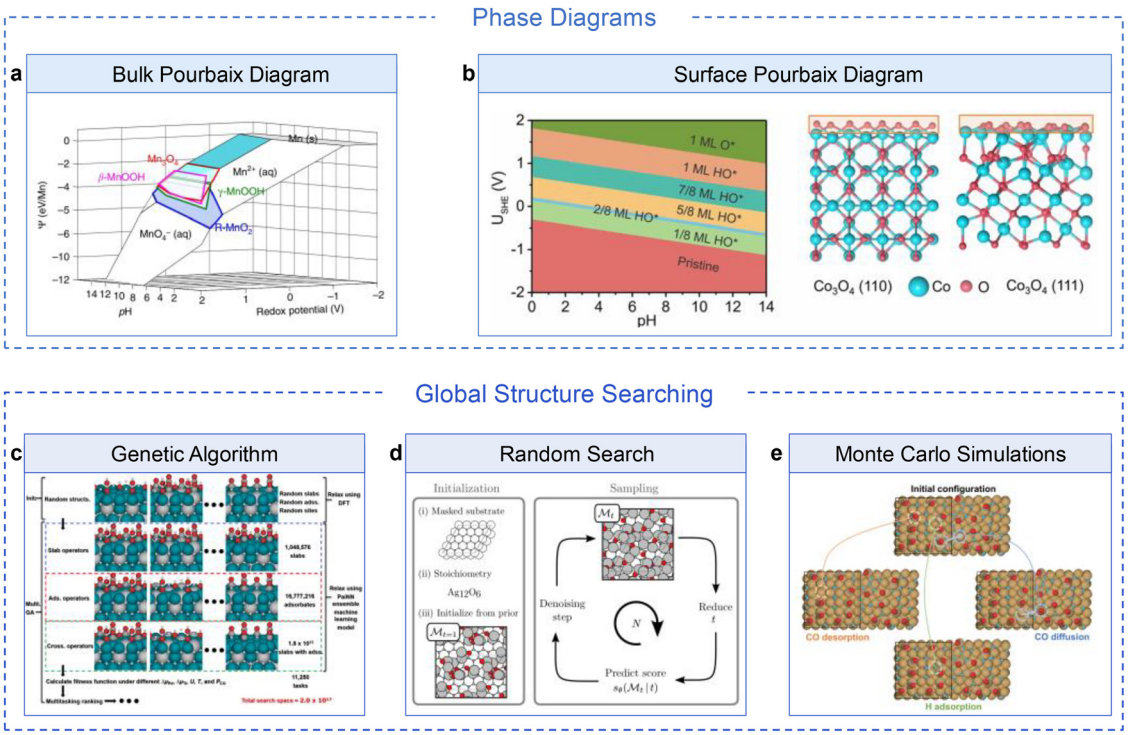

Fig. 2 Thermodynamic and global-optimization strategies for predicting electrocatalyst reconstruction. (a) Bulk Pourbaix diagram: Pourbaix free-energy planes of metastable β-MnOOH, γ-MnOOH and R-MnO_2, and the full aqueous stability region of Mn_3O_4. Adapted with permission from Sun *et al.* (CC BY 4.0).[33] (b) Surface Pourbaix diagram: calculated 2D surface Pourbaix diagrams for the (111) surface of H–Ir@Co_3O_4 as a function of potential and pH (T = 298.15 K). Adapted with permission from Wang *et al.* (CC BY 4.0).[34] (c) Genetic algorithm: process of global optimization for $Pd_xTi_{1-x}H_y$ with adsorbates CO*, H*, and OH* in the active learning workflow and the corresponding complexity. Adapted with permission from Ai *et al.* (Copyright © 2024 American Chemical Society.)[35] (d) Random search: sampling process exemplified with the p (4 × 4) AgO surface structure. The t = 1 structure is initialized at random using a prespecified substrate and a prespecified number and types of atoms. Adapted with permission from Rønne *et al.* (CC BY 4.0.)[36] (e) Monte Carlo: the schematic illustration of the typical attempted moves in quasi-kinetic Monte Carlo simulations. Adapted with permission from Zhang *et al.* (Copyright © 2024 American Chemical Society.)[37] No changes are made in all panels.

By capturing different surface terminations with various adsorbed intermediates and surface coverages (as a function of electrode potential and pH), surface Pourbaix diagrams could provide direct information for identifying reconstructed surface states under working conditions. For example, Wang and co-workers show that both (110) and (111) surfaces of spinel Co_3O_4 are covered by approximately 1 monolayer O* coverage at the oxygen evolution reaction (OER) potential (Fig. 2b).[34] Compared with the OH*-covered surface, O* passivates the surface-active sites and potentially contributes to the stability of Co_3O_4 in the acidic OER reaction.

Given the vast configurational space of reconstructed surfaces, manual enumeration of candidate structures can easily miss key metastable or kinetically accessible intermediates. This difficulty has motivated the development of global structure search techniques. Genetic algorithms (GAs), for example, are a classical approach that mimics natural selection by encoding structures as "genes" and iteratively evolving populations through selection, crossover, and mutation to identify energetically favorable configurations.[40,41] Ai and co-workers recently combined deep learning with a multitasking GA to screen $Pd_xTi_{1-x}H_y$ surfaces containing multiple adsorbates under different CO_2RR conditions (Fig. 2c),[35] where the configurational space includes variable Pd/Ti occupation of metal sites, internal hydrogen incorporation, and multiple adsorbate species distributed over inequivalent adsorption sites. For a 2 × 2 × 4 $Pd_xTi_{1-x}H_y$ slab model, a huge structural space with approximately 1.8×10^{13} structures is generated, arising from 2^{20} = 1 048 576 possible slab configurations and 4^{12} = 16 777 216 possible adlayer patterns. This GA approach can effectively identify low-energy and metastable configurations with varying compositions, hydrogen contents, and adsorbate environments. Therefore, data-guided global research helps explore reconstructed surface spaces beyond manually constructed structural models.

Another approach is random search, which generates candidate structures stochastically within a predefined space and evaluates them using energy calculations. Although potentially less efficient, it offers a simple method of globally exploring the complex configurational landscape. Rønne *et al.* performed random structure searching (RSS) on small Ag(111)-c(4 × 8) surface unit cells with varying stoichiometries (Fig. 2d).[36] After structural relaxation using DFT or machine-learning potentials, the lowest-energy configurations were selected to construct the training dataset for a generative model.

Furthermore, Monte Carlo (MC)-based simulations offer a useful framework for statistically exploring ensembles of atomic configurations at finite temperatures.[42–45] Trial configurations are sampled according to Boltzmann probabilities, enabling

evaluation of ensemble-averaged properties such as size-dependent surface energies, chemical potentials, and equilibrium shapes under realistic thermal conditions. For example, in quasi-kinetic MC simulations of CO_2 electroreduction on Cu surfaces, trial moves including atomic swaps, adsorption, and displacement were proposed from an initial surface configuration and evaluated using a DFT-derived energy model. Repeated sampling then generates a representative ensemble of surface structures, thereby enabling more efficient and comprehensive exploration of thermodynamically accessible reconstruction patterns and candidate structural evolution pathways at finite temperature (Fig. 2e).[37] By incorporating configurational entropy and morphological non-ideality, this methodology enables more realistic exploration of thermodynamically accessible reconstructed surface configurations.

Recent progress in high-performance computing, data-driven modeling, and machine learning algorithms has greatly expanded the scope of thermodynamic modeling of catalyst reconstruction.[31] In particular, MLPs now enable efficient and accurate exploration of high-dimensional configurational spaces that are prohibitive for direct DFT calculations. By training MLPs on curated DFT datasets, thousands to millions of surface configurations, including different surface terminations, adsorbate coverages, alloy compositions, and defect motifs, can be evaluated at near-DFT fidelity but with orders-of-magnitude reduced computational cost. When coupled with MC or related equilibrium sampling techniques, MLPs can extend static DFT-based analysis to finite-temperature ensemble predictions. Such workflows allow large numbers of configurations to be sampled as a function of composition, temperature, and chemical potential, thereby constructing new phase maps that explicitly account for configurational entropy and collective atomic rearrangements (Fig. 3a).[46]

In multicomponent alloy systems, this capability has been exploited to elucidate subtle yet experimentally relevant trends, such as facet-dependent surface segregation and size-dependent compositional redistribution in nanoparticles. As illustrated in Fig. 3b,[47] MLP-accelerated structure optimization enables equilibrium Wulff constructions of alloy nanoparticles containing thousands of atoms, yielding detailed composition profiles and facet-specific enrichment patterns that are inaccessible to brute-force DFT. Beyond configurational sampling, the accuracy and transferability of MLPs critically depend on how local atomic environments are represented, and such representational capacity becomes particularly important when exploring complex surface and interface reconstructions. Fig. 3c presents representative

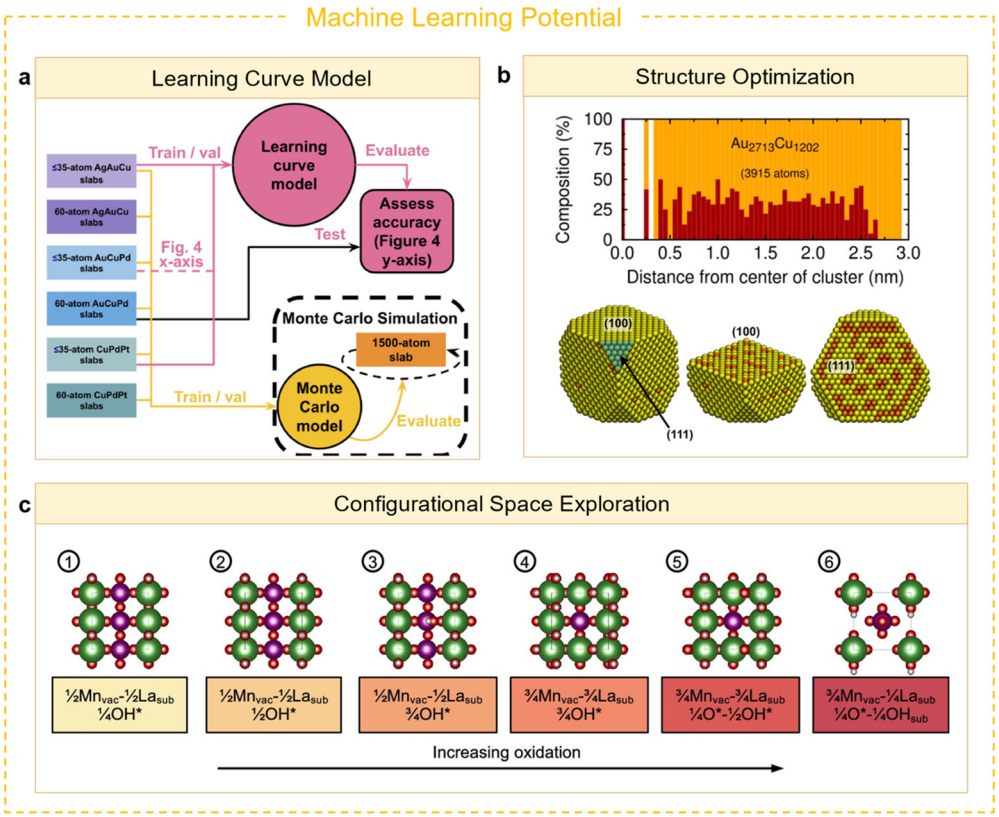

Fig. 3 The application of machine learning potential on static diagrams. (a) Learning curve model: a flowchart demonstrating how DFT data is used to construct learning curves for Monte Carlo simulations on AgAuCu, AuCuPd, and CuPdPt alloys. Adapted with permission from Broderick *et al.* (CC BY 4.0.)[46] (b) Structure optimization: composition of a Wulff constructing Cu/Au NP model with 3,915 atoms ($Au_{2713}Cu_{1202}$) and cut-throughs in the (100), and (111) directions. Adapted with permission from Artrith *et al.* (Copyright © 2014 American Chemical Society.)[47] (c) Configurational Space Exploration: $LaMnO_3$ (001) surface Pourbaix diagrams at pH 12 and across all ranges with newly discovered stable reconstructed surface states, generated after fine-tuning pre-trained MLPs with the DFT energetics of 136 surface structures. La, Mn, O, and H atoms are indicated by the green, purple, red, and white spheres, respectively. Adapted with permission from Du *et al.* (CC BY 4.0.)[48] Changes made: cropped to suit the distribution.

surface configurations among the stable $LaMnO_3(001)$ interfacial phases identified by the MLP-accelerated VSSR-MC search.[48] These structures feature mixed La/Mn terminations, metal vacancies, and variable adsorbate coverages. The large configuration space arising from variable surface stoichiometry, metal vacancy distribution, and OH* arrangements would require a prohibitive number of direct DFT calculations if each candidate structure were evaluated explicitly. To address this challenge, a high-fidelity MLP can be integrated into this structure-sampling framework of VSSR-MC as a surrogate energy model, enabling sampled surfaces to be evaluated on the fly rather than recalculated individually by DFT. This workflow couples automated sampling with fast DFT-trained MLP energy evaluation, making large-scale reconstruction searches more tractable.

By effectively bridging first-principles energetics and statistical thermodynamics, MLP-based approaches elevate static reconstruction modeling from comparisons among isolated structures to the ensemble-level and temperature-dependent thermodynamic predictions.[49–52] In this sense, they provide a critical foundation for subsequent kinetic simulations and multiscale modeling of electrocatalyst reconstruction.

2.2 Kinetic-based simulation of reconstruction

Although static calculation approaches establish thermodynamic equilibria and highlight competing structural motifs, *operando* reconstruction is often governed by kinetic accessibility and pathway dependence. Moreover, experimentally observed catalyzed behaviors, such as the persistence of metastable phases,[16] hysteresis in cyclic voltammetry profiles during surface oxidation/reduction,[53] and irreversible reconstruction,[54] remain inadequately explained by thermodynamics alone. Kinetic modeling is therefore indispensable for simulating time-dependent populations of surface species and interpreting phenomena such as hysteresis, metastability, induction periods, and path-selective transformations. Taking an example, *ab initio* molecular dynamics (AIMD)-based kinetic methods provide a direct route for probing atomistic reconstruction events by explicitly following atomic motions at finite temperature and capturing transient interfacial processes.[55–57] When combined with enhanced sampling, AIMD can further capture dynamic bond breaking and formation, surface-atom migration, and intermediate stabilization associated with elementary reconstruction steps. As shown in Fig. 4a, the free energy profile of Cu dissolution exhibits a strong dependence on the applied potential.[55] At −0.35 V *vs.* RHE, the free energy increases monotonically along the dissolution coordinate, indicating a substantial kinetic barrier that suppresses surface restructuring. As the reduction potential increases to −1.31 V *vs.* RHE, local minima emerge along the free-energy profile, reflecting the stabilization of intermediate states and facilitating metal dissolution and dynamic surface reorganization.

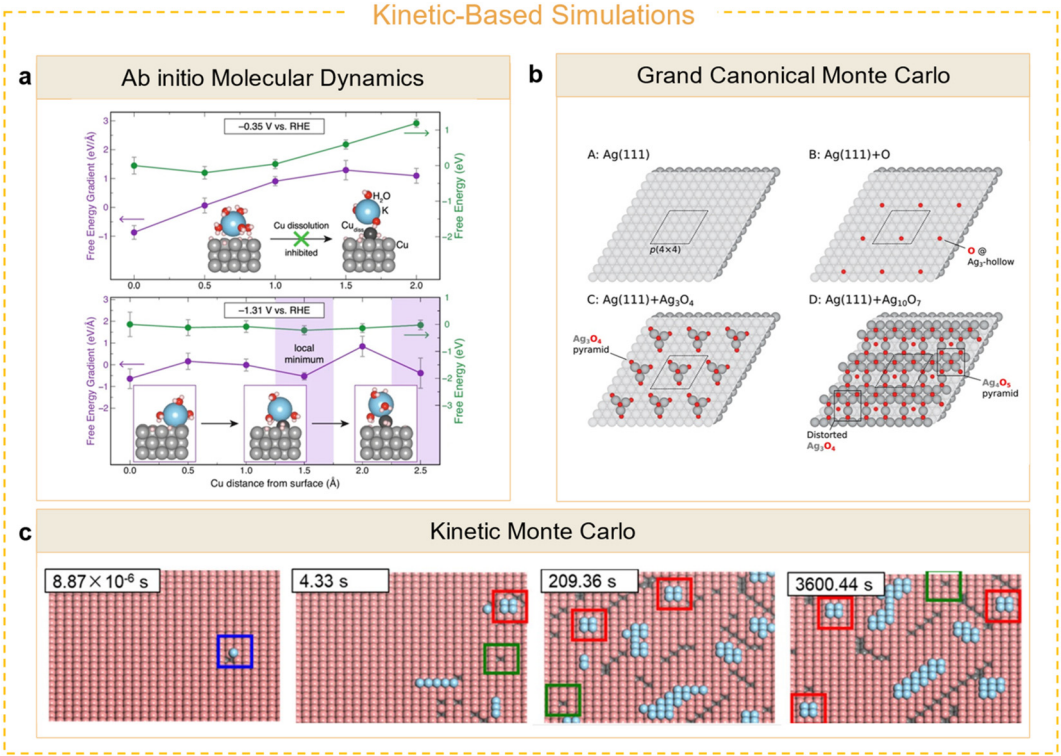

Fig. 4 Kinetic-based simulation approaches. (a) AIMD: free energy gradient (purple) and free energy (green) as functions of Cu distance from the surface along the coordinate of the dissolution reaction. Adapted with permission from Liu *et al.* (CC BY 4.0.)[55] (b) GCMC: Stable Ag (111) surfaces and reconstructions discovered by GCMC. Adapted with permission from Wexler *et al.* (Copyright © 2019 American Chemical Society.)[59] (c) kMC: environmental kinetic Monte Carlo snapshots of Cu (100) at 1-bar CO pressure, −0.2 V *vs.* RHE, and room temperature. Blue atoms represent atoms ejected from the surface. Pink atoms represent atoms on the surface. Gray atoms represent bulk atoms. Adapted with permission from Zhang *et al.* (Copyright © 2025 American Chemical Society.)[63] Changes made: cropped to suit the distribution.

AIMD is therefore complementary to static first-principles calculations, which are useful for evaluating predefined structures and reconstruction pathways but are limited in capturing time-dependent bond breaking, bond formation, and interfacial reorganization during reconstruction.

Grand-Canonical Monte Carlo (GCMC) further incorporates variable chemical potentials, thereby linking surface reconstruction to changes in the gas-phase or electrolyte environment.[58] In the previous study, GCMC was used to investigate the formation mechanism and phase diagram of oxide overlayers on the Ag(111) surface. As a result, the simulations revealed that a range of Ag(111) surface reconstructions could be understood on the basis of an Ag_3O_4 pyramidal structural motif, demonstrating that this approach can provide reliable atomic-scale modeling for studying complex surface processes such as heterogeneous catalysis and materials growth (Fig. 4b).[59] Kinetic Monte Carlo (kMC) simulations can extend accessible timescales to seconds or longer, beyond the practical limits of DFT and AIMD. Although first-principles calculations can probe individual elementary events and activation barriers, catalyst restructuring often emerges from the cumulative effect of many rare and repeated events, including diffusion, adsorption, desorption, surface atom migration, and chemical reaction steps.[60–62] By evolving a predefined event list with the corresponding rate constants derived from DFT or AIMD, kMC bridges atomistic reconstruction events with time-dependent changes in surface composition, morphology, and active-site redistribution. For example, Gao *et al.* used kMC simulation to reveal CO*-induced clustering on a Cu(100) surface in the CO_2RR (Fig. 4c).[63] Simulation results indicated the possibility of tuning the selectivity of the eCO_2RR reaction products through revealing the reconstruction mechanism on Cu(100) surfaces.[27,32]

Moreover, the integration of MLPs with kinetic simulation frameworks has fundamentally expanded the scope of dynamic modeling of catalyst reconstruction. By providing near first-principles accuracy at a fraction of the computational cost, MLP-based approaches enable long-timescale and interface-sensitive simulations that are inaccessible to conventional *ab initio* methods. Fig. 5 summarizes representative ML paradigms for kinetic modeling that address key bottlenecks in reconstruction dynamics, ranging from general kinetic diagrams to interfacial event identification and reaction pathway exploration.

In particular, MLPs serve as an enabling layer for kinetic modeling by coupling DFT data generation, active learning, and

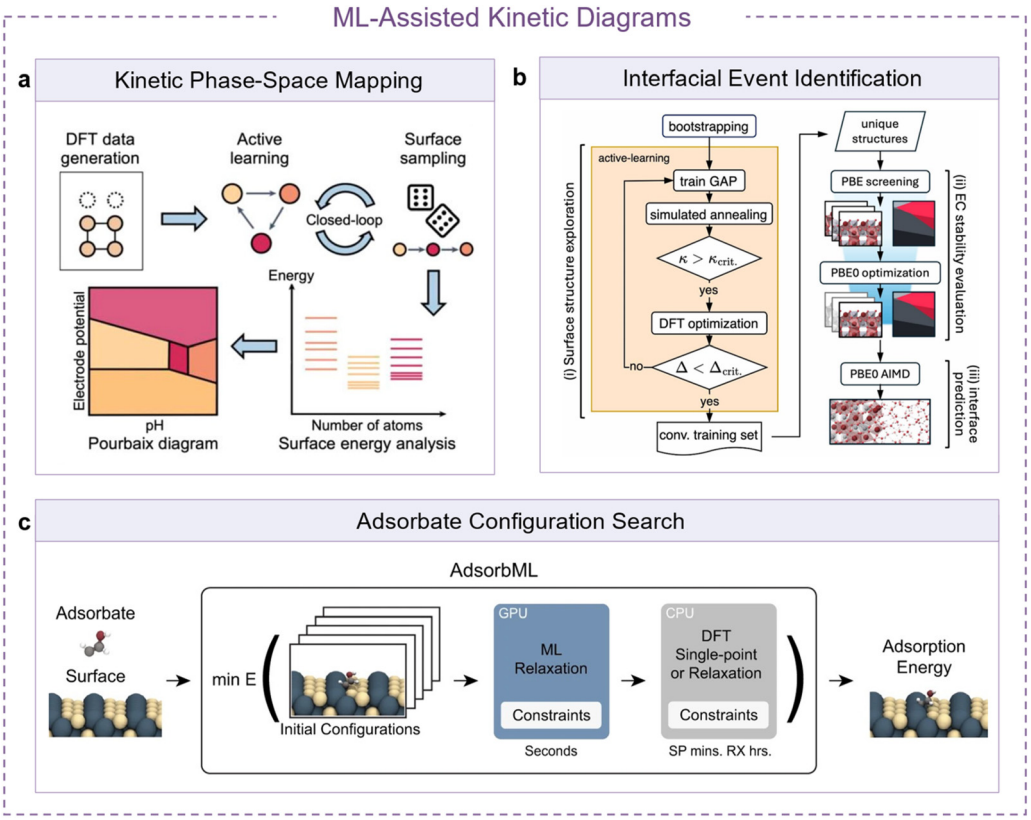

Fig. 5 Machine learning-assisted multiple kinetic diagrams. (a) Kinetic phase-space mapping: indication of the MLP application in kinetic diagrams. Adapted with permission from Du *et al.* (CC BY 4.0.)[64] (b) Interfacial event identification: computational workflow for structure exploration, stability evaluations of reconstructed $BiVO_4$ (010) surfaces, and prediction of dynamical properties at the aqueous interfaces of $BiVO_4$ (010). Adapted with permission from Lee *et al.* (Copyright © 2025 American Chemical Society.)[65] (c) Adsorbate configuration search: Initial configurations are generated *via* heuristic and random strategies. ML relaxations are performed on GPUs and ranked in order of lowest to highest energy. The best k systems are passed on to DFT for either a single-point (SP) evaluation or a full relaxation (RX) from the ML-relaxed structure. Adapted with permission from Lan *et al.* (CC BY 4.0.)[66] No changes are made in all panels.

surface sampling within a closed-loop workflow, thereby facilitating the construction of kinetic phase diagrams and surface stability maps under realistic electrochemical conditions (Fig. 5a).[64] Such general ML-assisted workflows illustrate how MLPs bridge first-principles energetics with statistical sampling, facilitating evaluation of surface energies, atomic populations, and stability trends across large configurational spaces that are otherwise prohibitive for direct DFT calculations.

A more explicit role of MLPs emerges in resolving reconstruction-initiating interfacial events, where accuracy at chemically complex interfaces is essential. In Fig. 5b,[65] active-learning-driven MLP workflows have been employed to explore reconstructed oxide surfaces at aqueous interfaces, as exemplified by the $BiVO_4$(010) system. In this paradigm, surface structures are iteratively generated and screened using MLP-accelerated sampling, followed by stability evaluation with density functional theory and hybrid-functional optimization. The resulting refined training sets enable reliable prediction of interfacial dynamical properties through molecular dynamics simulations. This approach allows key interfacial events, such as water dissociation, surface hydroxylation, and transient coordination changes, to be identified directly from dynamic trajectories, thereby providing mechanistic insights into the initiation of reconstruction under electrochemical conditions.

Beyond interfacial event identification, machine learning potentials also play a central role in efficient exploration of adsorption configurations and reaction-relevant structures on catalytic surfaces. In Fig. 5c, recent developments such as the Adsorb ML framework employ graph neural network-based potentials to rapidly relax large ensembles of adsorbate-surface configurations with near-DFT accuracy.[66] In this workflow, candidate structures are first generated and pre-screened based on their initial energies, followed by ML-driven structural relaxation under physically motivated constraints. The refined configurations can then be selectively evaluated using high-fidelity DFT calculations to obtain adsorption energies and reaction descriptors.

Collectively, these ML-assisted kinetic paradigms demonstrate that ML provides a coherent energetic foundation for kinetic modeling across interfaces, pathways, and time scales. In particular, they define the practical boundaries of reconstruction modeling, allowing atomic-scale events, interfacial dynamics, and pathway-dependent kinetics to be treated within a unified and operando-relevant computational description.[31,67]

Overall, phase-diagram approaches provide insight into thermodynamically stable structures under given electrochemical conditions but do not capture kinetic accessibility. In contrast, atomistic dynamics methods such as AIMD could explicitly describe structural evolution with high accuracy, but their accessible time and length scales remain limited. Mesoscale approaches such as kMC extend simulations to experimentally relevant timescales by propagating elementary events according to their rates, but rely on predefined reaction networks and corresponding rate constants. Meanwhile, GCMC enables treatment of open systems with variable composition under chemical potential control, although it primarily samples equilibrium or quasi-equilibrium configurations rather than real-time dynamics. Notably, MLPs bridge these regimes by enabling large-scale configurational sampling and long-time dynamical simulations with near first-principles accuracy, thereby providing a unified framework for investigating electrocatalyst reconstruction across multiple scales. In this process, MLPs play a dual role in reconstruction modeling: they can be used for efficient thermodynamic sampling of complex configurational spaces, while also enabling accelerated atomistic dynamics to capture long-timescale kinetic processes. Together, these approaches form a complementary multiscale computational framework capable of predicting not only what a catalyst may become, but how and when it transforms under operating conditions. A comparative summary of these approaches is provided in Table 1 to guide their practical application.

In reconstruction modeling, MLPs can be integrated with various simulation methods to accelerate configurational sampling and dynamic evolution while achieving DFT-level energetics within the trained domain. However, the main computational bottleneck in MLP applications has shifted to generating high-fidelity first-principles datasets for training and validation. The reconstruction process involves large supercells, complex interfacial environments, defect formation, adsorbate variability, surface atom migration, and long-time trajectories. Therefore, constructing DFT-based datasets for complex, non-equilibrium reconstruction events remains particularly expensive. Rare transition states and metastable intermediates are often underrepresented, increasing the risk of extrapolation.[68] Operando validation is also limited by ensemble-averaged or indirect structural information. Future efforts should therefore combine active learning, uncertainty-aware sampling, targeted rare-event sampling, and closer integration with operando characterization to improve dataset coverage and model validation.[69]

3 Outlook and conclusion

Computational studies for electrocatalyst reconstruction have advanced from static thermodynamic analysis to increasingly dynamic and multi-scale simulations, enabling a more detailed description of structural evolution from atomic-scale mechanisms to system-level evolution. However, when addressing dynamic reconstruction in complex open systems such as electrocatalysis, two distinct but interconnected methodological challenges remain: (1) explicitly describing reconstruction as an environment-coupled open-system process; and (2) bridging the gap between atomic-scale events and electrode-scale operating conditions across multiple spatial and temporal scales.

3.1 Developing kinetic models for environment-coupled open-system reconstruction

Most existing phase diagrams and kinetic approaches inherently treat systems as 'closed', focusing mainly on atomic rearrangement or local stoichiometric changes.[31,33,34] In practical electrocatalytic systems, however, reconstruction is dynamically coupled to the surrounding electrochemical environment through continuous

Table 1 Comparison of computational approaches for electrocatalyst reconstruction modeling, including their advantages, limitations, and characteristic time and length scales. AIMD, *ab initio* molecular dynamics; kMC, kinetic Monte Carlo; GCMC, grand-canonical Monte Carlo; MLP, machine-learning potential

Method	Advantages	Limitations	Time scale	Length scale
Phase diagrams (*e.g.*, Pourbaix)	Identify thermodynamically stable phases under electrochemical conditions; straightforward to construct	Do not account for kinetics or metastable states	Equilibrium (static)	nm–μm
AIMD	Explicit atomistic dynamics with first-principles accuracy; captures bond breaking/forming and solvent effects	High computational cost; limited to short timescales	ps–ns	Å–nm
GCMC	Naturally treats open systems with variable composition; suitable for adsorption/desorption equilibria	Limited description of real-time dynamics; requires predefined chemical potentials	quasi-static/sampling-based	nm
kMC	Enables long-time evolution and rare-event sampling; suitable for kinetic processes	Requires predefined reaction network and rate constants; accuracy depends on input parameters	μs–s (or longer)	nm–μm
MLP-based methods	Near-DFT accuracy with significantly reduced cost; enables large-scale sampling and long-time simulations	Requires high-quality training data; transferability may be limited	ps–μs (extendable)	nm–100 nm

exchange of matter, charge, and chemical potential. Recent studies have highlighted that electrocatalyst reconstruction is inherently an open-system process, where structural evolution is strongly coupled with the surrounding electrolyte environment. In particular, dissolution–redeposition dynamics, together with interfacial ion distributions, can dynamically modify local chemical potentials and surface stability, thereby influencing reconstruction pathways under operating conditions. For instance, Vavra *et al.* demonstrated that Cu^+ species formed in solution can act as mobile intermediates, continuously dissolving from and redepositing onto the catalyst surface, thereby driving dynamic restructuring beyond a purely surface-confined process.[70] Extending this concept, Kim *et al.* revealed that such dissolution–redeposition behavior in Cu-based bimetallic systems can be systematically governed by metal oxophilicity and miscibility, establishing a predictive framework for reconstruction pathways.[71] Complementarily, multiscale simulations in Kok *et al.* highlighted that local electrolyte microenvironments, including ion distributions and pH gradients, can dynamically modulate surface stability and reaction energetics.[72] Together, these studies underscore that catalyst reconstruction emerges from the interplay between surface processes and a continuously evolving electrochemical environment. This open-system character is manifested not only in dissolution-redeposition, but also in adsorbate exchange, ion accumulation, local pH variation, electric-field effects, and mass transport near the catalyst-electrolyte interface.[9–13] As a result, reconstruction cannot be fully described as an intrinsic surface process alone, but must instead be understood as an environment-coupled dynamic response under operating conditions.

Future progress will therefore require kinetic frameworks that explicitly incorporate the evolving local environment into reconstruction modeling. One promising direction is to extend event-based simulations to include environment-dependent processes, such as metal dissolution/redeposition, adsorbate adsorption/desorption, and ion-coupled surface transformation.

Simultaneously, the grand-canonical ensemble concept extends from electron/adsorbate chemical potentials to those of dissolved metal ions, thereby dynamically linking microscopic reconstruction events to macroscopic electrolyte concentration fields, electric fields, and mass transport. Such open-system kinetic models will provide a more realistic basis for predicting catalyst morphology evolution, active area changes, and stability decay under given operating conditions.

3.2 Building a unified multi-scale computational model for reconstruction

Atomistic simulations can reveal site-specific events and elementary steps, but they are difficult to connect directly to macroscopic variables, such as local current density, pH, and ion concentration. Conversely, continuum or device-level models capture system-level behavior under operating conditions. Therefore, bridging the microscopic mechanisms and macroscopic behaviors is both essential and challenging for more realistic simulations across practical length scales and operating conditions.[31] Recent multiscale studies have begun to explicitly bridge this gap by integrating atomistic energetics with macroscopic observables. For example, Shou *et al.* developed a multiscale framework that links first-principles-derived reaction energetics with microkinetic modeling to reproduce experimentally observed polarization curves, thereby directly connecting atomic-scale mechanisms with current–potential behavior.[73] In parallel, Lorenzutti *et al.* demonstrated that coupling surface reaction kinetics with electrolyte transport and interfacial ion distributions can quantitatively capture the impact of local microenvironments on activity and selectivity.[74] These advances highlight the necessity of incorporating both kinetic and environmental complexities to achieve predictive multiscale modeling.

Consequently, computationally tractable multiscale frameworks are needed to bridge the atom–nano–micro–device scales in a unified manner. The Hierarchical Modeling Strategy (HMS)

that combines atomistic simulations, machine-learned potentials, coarse-grained force fields, and continuum methods may provide an effective route for parameter transfer and feedback mechanisms across scales. Recent studies have gradually demonstrated the feasibility of this direction.[73,74] Focusing on the catalyst reconstruction modeling, the multiscale model should further incorporate environment-embedded simulations that explicitly couple local electric fields, ionic strength, and reactant concentration gradients into dynamic simulations,[75] thereby providing more realistic guidance for understanding and controlling catalyst behaviors under practical operating conditions.

3.3 Conclusion

Computational approaches have become indispensable for studying electrocatalyst reconstruction, enabling increasingly detailed descriptions of structural evolution under operating conditions. By combining thermodynamic analysis, kinetic simulations, and multiscale modeling, current computational approaches can already capture some key aspects of reconstruction across different length and time scales. Looking ahead, developing open-system kinetic models and constructing unified multiscale computational frameworks will move catalyst reconstruction studies closer to practical catalyst evaluation and predictive simulations. Given the complexity and dynamic features of the electrocatalysis environment, achieving this goal will require tight integration of computational modeling with electrochemical theory, data-driven methods, and operando characterization.

Author contributions

X.-Y. L. conceived and supervised the project and guided the overall structure, content development, and revision of the paper. Z. L. conducted the literature survey, prepared the figures, and drafted the manuscript.

Conflicts of interest

There are no conflicts to declare.

Data availability

Data availability is not applicable to this article as no new data were created or analyzed in this study.

Acknowledgements

X.-Y. L. acknowledges the support from the National University of Singapore Start-Up Grant (grant A-0010269-00-00) and the Ministry of Education, Singapore, under Academic Research Fund Tier 1 (grant A-8004135-00-00).

References

1 Z. Yang, M. Xiang, H. Niu, X. Xie, C. Yu, J. Hui and S. Dong, *J. Solid State Chem.*, 2022, **314**, 123365, DOI: 10.1016/j.jssc.2022.123365.
2 A. K. Nayak and D. Pradhan, *ACS Appl. Energy Mater.*, 2025, **8**, 2088–2102, DOI: 10.1021/acsaem.4c02585.
3 F. Vieira, P. Marcasuzaa, L. Curet, L. Billon, A. Viterisi and E. Palomares, *ACS Appl. Mater. Interfaces*, 2024, **16**, 45038–45048, DOI: 10.1021/acsami.4c11927.
4 A. Johnpaul, A. Vijayaprabhakaran, M. Krishnan and M. Kathiresan, *Energy Fuels*, 2024, **38**, 18844–18852, DOI: 10.1021/acs.energyfuels.4c03129.
5 D. A. Chipoco Haro, L. Barrera, H. Iriawan, A. Herzog, N. Tian, A. J. Medford, Y. Shao-Horn, F. M. Alamgir and M. C. Hatzell, *ACS Catal.*, 2024, **14**, 9752–9775, DOI: 10.1021/acscatal.4c01398.
6 Z. Shen, F. Xu, X. Cheng, J. Jiang, C. Zhou, Y. Zeng, X. Z. Wang, L. Yang, Q. Wu and Z. Hu, *ACS Nano*, 2025, **19**, 4611–4621, DOI: 10.1021/acsnano.4c14802.
7 C. Li, Y. Kawamata, H. Nakamura, J. C. Vantourout, Z. Liu, Q. Hou, D. Bao, J. T. Starr, J. Chen, M. Yan and P. S. Baran, *Angew. Chem., Int. Ed.*, 2017, **56**, 13088–13093, DOI: 10.1002/anie.201707906.
8 Y. Wang, F. Zhang, Y. Wang and Y. Pan, *Eur. J. Org. Chem.*, 2022, e202101462, DOI: 10.1002/ejoc.202101462.
9 J. Li, H. Tan, J. Jia, C. Wang, W. Hao, X. Yan, W. Si, Y. Tian, F. Hou, L. Yin and J. Liang, *J. Energy Chem.*, 2026, **115**, 54–64, DOI: 10.1016/j.jechem.2025.11.013.
10 I. Furrick, A. Omoniyi, S. Wang, T. Robinson and A. J. R. Hensley, *ChemCatChem*, 2024, **16**, e202400551, DOI: 10.1002/cctc.202400551.
11 H. Dai, L. Gomes, D. Maxwell, S. Zamani, K. Yang, D. Atienza, N. Dale and S. Mukerjee, *ACS Appl. Mater. Interfaces*, 2024, **16**, 8639–8654, DOI: 10.1021/acsami.3c15670.
12 Y.-G. Kim, J. H. Baricuatro and M. P. Soriaga, *Electrocatalysis*, 2018, **9**, 526–530, DOI: 10.1007/s12678-018-0469-z.
13 B. Tomc, M. Bele, M. Plut, M. Kostelec, S. Popovic, M. A. Nazrulla, F. Ruiz-Zepeda, A. R. Kamsek, M. Sala, A. Elbataioui, L. D. Rafailovic, Y. B. Pissolitto, F. Trivinho-Strixino, W. J. Stepniowski, L. Suhadolnik and N. Hodnik, *J. Phys. Chem. Lett.*, 2025, **16**, 9553–9560, DOI: 10.1021/acs.jpclett.5c01974.
14 M. Kang, H. B. Jeong, Y. Shim, H. J. Chai, Y. S. Kim, M. Choi, A. Ham, C. Park, M. K. Jo, T. S. Kim, H. Park, J. Lee, G. Noh, J. Y. Kwak, T. Eom, C. W. Lee, S. Y. Choi, J. M. Yuk, S. Song, H. Y. Jeong and K. Kang, *ACS Nano*, 2024, **18**, 819–828, DOI: 10.1021/acsnano.3c09369.
15 H. Xue, W. Zhao, M. Zhan, D. Zhou, N. Zhang, Z. Chen, R. Qi, M. Chu, S. Li, J. Wang, Q. Liu, F. Pan and M. Zhang, *ACS Nano*, 2026, **20**, 7205–7215, DOI: 10.1021/acsnano.5c20611.
16 W. Pang, X. Du, Y. Yang, C. Long, Y. Li, C. Hu, R. Xu, M. Tian, J. Xie, W. Wang, J. Guo, B. Li, P. Zhang, D. Fu and K. Zhao, *Adv. Funct. Mater.*, 2024, **34**, 2400466, DOI: 10.1002/adfm.202400466.
17 Y. Cao, Y. Zhao, T. Tang, S. Cui, M. Li, X. Sun, W. Cui and H. Zhao, *Chem. Eng. J.*, 2025, **522**, 167200, DOI: 10.1016/j.cej.2025.167200.
18 M. Kempasiddaiah, R. Samanta, S. Panigrahy, R. K. Trivedi, B. Chakraborty and S. Barman, *Nanoscale*, 2024, **16**, 10458–10473, DOI: 10.1039/d4nr00824c.
19 W. Ni, Y. Zhou, Y. Yao, X. Wang, R. Zhao, Z. Yang, X. Li and Y.-M. Yan, *ACS Appl. Mater. Interfaces*, 2022, **14**, 13261–13270, DOI: 10.1021/acsami.1c23662.
20 W. Tu, K. Chen, L. Zhu, H. Zai, X. Ke, C. Chen, M. Sui, Q. Chen and Y. Li, *Adv. Funct. Mater.*, 2019, **29**, 1807070, DOI: 10.1002/adfm.201807070.
21 C. Yang, W. Ling, Y. Zhu, Y. Yang, S. Dong, C. Wu, Z. Wang, S. Yang, J. Li, G. Wang, Y. Huang, B. Yang, Q. Cheng, Z. Liu and H. Yang, *Appl. Catal. B Environ.*, 2024, **358**, 124462, DOI: 10.1016/j.apcatb.2024.124462.
22 J. Sun, Z. Xu, D. Liu, A. Kong, Q. Zhang and R. Liu, *Chin. J. Catal.*, 2025, **72**, 112–122, DOI: 10.1016/S1872-2067(24)60287-1.
23 Y. Fan, S. Zhang, X. Ye, J. Zhou, Q. Kong, J. Zhang, Y. Long, J. Q. Wang, Z. Hu and L. Zhang, *InfoMat*, 2025, **7**, e70053, DOI: 10.1002/inf2.70053.
24 D. Liu, H. Ai, J. Li, M. Fang, M. Chen, D. Liu, X. Du, P. Zhou, F. Li, K. H. Lo, Y. Tang, S. Chen, L. Wang, G. Xing and H. Pan, *Adv. Energy Mater.*, 2020, **10**, 2002464, DOI: 10.1002/aenm.202002464.
25 C. O. Ogolla, M. Kasper, M. F. Puthiyaparambath, N. Farahbakhsh, R. Thapa, M. Thandavarayan, M. S. Killian, B. Butz and J. M. V. Nsanzimana, *Small*, 2025, **21**, e07475, DOI: 10.1002/smll.202507475.
26 C. Chen, C. Du, Z. Wang, X. Chen, Y. Wang, N. Ju, Y. Fu, Z. Liu, M. Jia, S. Luo, G. Xu, J. Xu and H.-B. Sun, *Energy & Fuels*, 2025, **39**, 12154–12164, DOI: 10.1021/acs.energyfuels.5c01693.
27 Z. Guo, Y. Yu, C. Li, E. Campos Dos Santos, T. Wang, H. Li, J. Xu, C. Liu and H. Li, *Angew. Chem., Int. Ed.*, 2024, **63**, e202319913, DOI: 10.1002/anie.202319913.

28 A. J. Martin, S. Mitchell, C. Mondelli, S. Jaydev and J. P. Ramírez, *Nat. Catal.*, 2022, **5**, 854–866, DOI: 10.1038/s41929-022-00842-y.
29 X. Liu, K. Park, M. So, S. Ishikawa, T. Terao, K. Shinohara, C. Komori, N. Kimura, G. Inoue and Y. Tsuge, *J. Power Sources Adv.*, 2022, **14**, 100084, DOI: 10.1016/j.powera.2022.100084.
30 Y. Wang, L. Zhou, X. Yin, X. Liu, X. Fu, Y. Wang and Z. Liu, *Chem. Eng. J.*, 2025, **525**, 170688, DOI: 10.1016/j.cej.2025.170688.
31 J. Peng, *J. Chem. Phys.*, 2025, **163**, 040902, DOI: 10.1063/5.0271797.
32 Y. Wang, D. Zhang, B. Sun, X. Jia, L. Zhang, H. Cheng, J. Fan and H. Li, *Angew. Chem., Int. Ed.*, 2025, **64**, e202418228, DOI: 10.1002/anie.202418228.
33 W. Sun, D. A. Kitchaev, D. Kramer and G. Ceder, *Nat. Commun.*, 2019, **10**, 573, DOI: 10.1038/s41467-019-08494-6.
34 Y. Wang, Y. Qin, S. Liu, Y. Zhao, L. Liu, D. Zhang, S. Zhao, J. Liu, J. Wang, Y. Liu, H. Wu, B. Jia, X. Qu, H. Li and M. Qin, *J. Am. Chem. Soc.*, 2025, **147**, 13345–13355, DOI: 10.1021/jacs.4c18390.
35 C. Ai, S. Han, X. Yang, T. Vegge and H. A. Hansen, *ACS Appl. Mater. Interfaces*, 2024, **16**, 12563–12572, DOI: 10.1021/acsami.3c18734.
36 N. Rønne, A. Aspuru-Guzik and B. Hammer, *Phys. Rev. B*, 2024, **110**, 235427, DOI: 10.1103/PhysRevB.110.235427.
37 Z. Zhang, W. Gee, P. Sautet and A. N. Alexandrova, *J. Am. Chem. Soc.*, 2024, **146**, 16119–16127, DOI: 10.1021/jacs.4c03515.
38 I. T. McCrum, M. A. Hickner and M. J. Janik, *Langmuir*, 2017, **33**, 7043–7052, DOI: 10.1021/acs.langmuir.7b01530.
39 C. Griesser, H. Li, E. M. Wernig, D. Winkler, N. Shakibi Nia, T. Mairegger, T. Gotsch, T. Schachinger, A. Steiger-Thirsfeld, S. Penner, D. Wielend, D. Egger, C. Scheurer, K. Reuter and J. Kunze-Liebhauser, *ACS Catal.*, 2021, **11**, 4920–4928, DOI: 10.1021/acscatal.1c00415.
40 Z. Yang, Z. Ni, X. Li, X. Wang, K. Han and Y. Wang, *Int. J. Hydrogen Energy*, 2025, **100**, 829–840, DOI: 10.1016/j.ijhydene.2024.11.079.
41 M. Ayatizadeh Tanha, M. Kazemeini, V. Hosseinpour and F. Raji, *Results Eng.*, 2025, **27**, 105784, DOI: 10.1016/j.rineng.2025.105784.
42 C. Pareige, M. Roussel, S. Novy, V. Kuksenko, P. Olsson, C. Domain and P. Pareige, *Acta Mater.*, 2011, **59**, 2404–2411, DOI: 10.1016/j.actamat.2010.12.038.
43 K. H. Mali, R. Pokar and A. Dashora, *J. Mater. Chem. A*, 2025, **13**, 2859–2874, DOI: 10.1039/d4ta07462a.
44 L. V. Lutsevich, V. I. Elokhin and G. S. Yablonskii, *Kinet. Catal. Lett.*, 1993, **51**, 269–277, DOI: 10.1007/BF02069067.
45 S. Döpling and S. Matera, *Chem. Phys. Lett.*, 2017, **674**, 28–32, DOI: 10.1016/j.cplett.2017.02.043.
46 K. Broderick, R. A. Burnley, A. J. Gellman and J. R. Kitchin, *Chem. Phys. Chem.*, 2024, **25**, e202400073, DOI: 10.1002/cphc.202400073.
47 N. Artrith and A. M. Kolpak, *Nano Lett.*, 2014, **14**, 2670–2676, DOI: 10.1021/nl5005674.
48 X. Du, M. Liu, J. Peng, H. Chun, A. Hoffman, B. Yildiz, L. Li, M. Z. Bazant and R. Gomez-Bombarelli, *ACS Cent. Sci.*, 2025, **11**, 1558–1572, DOI: 10.1021/acscentsci.5c00547.
49 P. Hou, Q. Yu, F. Luo and J.-C. Liu, *ACS Catal.*, 2025, **15**, 352–360, DOI: 10.1021/acscatal.4c05338.
50 X. Cheng, C. Wu, J. Xu, Y. Han, W. Xie and P. Hu, *Precis. Chem.*, 2024, **2**, 570–586, DOI: 10.1021/prechem.4c00051.
51 Y. Han, J. Xu, W. Xie, Z. Wang and P. Hu, *ACS Catal.*, 2023, **13**, 5104–5113, DOI: 10.1021/acscatal.3c00658.
52 S. Ma, S. Wang, S. Wang, X. Chen, H. He, X. Zhang, S. Zhai, Q. Han, P. Zhang, K. Zi, N. Yan, Y. Tie, D. Ding, X. Chen, Y. Zhao, M. Ye, A. N. Alodhayb, Z. Chen, Y. Zheng, J. Li and Y. Sun, *ACS Catal.*, 2025, **15**, 20560–20572, DOI: 10.1021/acscatal.5c06762.
53 M. Tian and B. E. Conway, *J. Electroanal. Chem.*, 2008, **616**, 45–56, DOI: 10.1016/j.jelechem.2007.12.016.
54 H.-Y. Chen, Y. Lugo-Jose, J. M. Fedeyko, T. J. Toops and J. Fidler, *ACS Catal.*, 2024, **14**, 15751–15763, DOI: 10.1021/acscatal.4c03690.
55 S. Liu, Y. Li, D. Wang, S. Xi, H. Xu, Y. Wang, X. Li, W. Zang, W. Liu, M. Su, K. Yan, A. C. Nielander, A. B. Wong, J. Lu, T. F. Jaramillo, L. Wang, P. Canepa and Q. He, *Nat. Commun.*, 2024, **15**, 5080, DOI: 10.1038/s41467-024-49492-7.
56 S. Praserthdam and P. B. Balbuena, *Catal. Sci. Technol.*, 2016, **6**, 5168–5177, DOI: 10.1039/c5cy02287h.
57 Y. Yang, M. Jiang, S. Xiao, S. Tang, S. Zhong, H. Li and B. Liang, *Langmuir*, 2025, **41**, 14019–14026, DOI: 10.1021/acs.langmuir.5c00887.
58 J. L. Li, Y. F. Li and Z. P. Liu, *JACS Au*, 2023, **3**, 1162–1175, DOI: 10.1021/jacsau.3c00038.
59 R. B. Wexler, T. Qiu and A. M. Rappe, *J. Phys. Chem. C*, 2019, **123**, 2321–2328, DOI: 10.1021/acs.jpcc.8b11093.
60 A. L. Lloyd, R. Smith and S. D. Kenny, *J. Mater. Res.*, 2018, **33**, 847–856, DOI: 10.1557/jmr.2017.482.
61 J. Li, G. Liu, B. Ren, E. Croiset, Y. Zhang and L. Ricardez-Sandoval, *J. Catal.*, 2019, **378**, 176–183, DOI: 10.1016/j.jcat.2019.08.029.
62 D. S. D. Gunn, N. L. Allan and J. A. Purton, *J. Mater. Chem. A*, 2014, **2**, 13407–13414, DOI: 10.1039/c4ta01504e.
63 S. Zhang, Q. Tang, B. Zhu and Y. Gao, *ACS Catal.*, 2025, **15**, 6497–6506, DOI: 10.1021/acscatal.4c07168.
64 X. Du, J. K. Damewood, J. R. Lunger, R. Millan, B. Yildiz, L. Li and R. Gomez-Bombarelli, *Nat. Comput. Sci.*, 2023, **3**, 1034–1044, DOI: 10.1038/s43588-023-00571-7.
65 Y. Lee and T. Lee, *J. Am. Chem. Soc.*, 2025, **147**, 7799–7808, DOI: 10.1021/jacs.4c17739.
66 J. Lan, A. Palizhati, M. Shuaibi, B. M. Wood, B. Wander, A. Das, M. Uyttendaele, C. L. Zitnick and Z. W. Ulissi, *npj Comput. Mater.*, 2023, **9**, 172, DOI: 10.1038/s41524-023-01121-5.
67 J. Behler, *J. Chem. Phys.*, 2016, **145**, 170901, DOI: 10.1063/1.4966192.
68 L. Bonati, G. Piccini and M. Parrinello, *Proc. Natl. Acad. Sci. U.S.A.*, 2021, **118**, e2113533118, DOI: 10.1073/pnas.2113533118.
69 K. Zhu, E. Trizio, J. Zhang, R. Hu, L. Jiang, T. Hou and L. Bonati, *Chem. Rev.*, 2026, **126**, 671–713, DOI: 10.1021/acs.chemrev.5c00700.
70 J. Vavra, G. P. L. Ramona, F. Dattila, A. Kormányos, T. Priamushko, P. P. Albertini, A. Loiudice, S. Cherevko, N. Lopez and R. Buonsanti, *Nat. Catal.*, 2024, **7**, 89–97, DOI: 10.1038/s41929-023-01070-8.
71 I. Kim, G. B. Lee, S. Kim, H. D. Jung, J. Y. Kim, T. Lee, H. Choi, J. Jo, G. Kang, S. H. Oh, W. Kwon, D. Hong, H. G. Kim, Y. Lee, U. Kim, H. Kim, M. Kim, S. Back, J. Park, Y. C. Joo and D. H. Nam, *Nat. Catal.*, 2025, **8**, 697–713, DOI: 10.1038/s41929-025-01368-9.
72 J. Kok, P. P. Albertini, J. Leemans, R. Buonsanti and T. Burdyny, *Nat. Rev. Mater.*, 2025, **10**, 550–563, DOI: 10.1038/s41578-025-00815-0.
73 W. Shou, W. Zhao, Y. Liu and T. Wang, *Nat. Commun.*, 2025, **17**, 802, DOI: 10.1038/s41467-025-67493-y.
74 F. Lorenzutti, R. R. Seemakurthi, E. F. Johnson, S. Morandi, P. Nikacevic, N. Lopez and S. Haussener, *Nat. Catal.*, 2025, **8**, 905–918, DOI: 10.1038/s41929-025-01399-2.
75 M. S. Shahreza, S. Sogbaike, A. Archibong-Eso, I. M. Albayati and A. M. Aliyu, *J. Energy Resour. Technol., Part A*, 2025, **1**, 061703, DOI: 10.1115/1.4069226.

